The Mass Of The Coma Cluster From Weak Lensing In The Sloan Digital Sky Survey

Jeffrey M. Kubo[1], Albert Stebbins[1], James Annis[1], Ian P. Dell'Antonio[2], Huan Lin[1], Hossein Khiabanian[2], Joshua A. Frieman [1,3]

ABSTRACT

We present a weak lensing analysis of the Coma Cluster using the Sloan Digital Sky Survey (SDSS) Data Release Five. Complete imaging of a ~ 200 square degree region is used to measure the tangential shear of this cluster. The shear is fit to an NFW model and we find a virial radius of $r_{200} = 1.99^{+0.21}_{-0.22}\mathrm{h}^{-1}\mathrm{Mpc}$ which corresponds to a virial mass of $M_{200} = 1.88^{+0.65}_{-0.56} \times 10^{15}\mathrm{h}^{-1}\mathrm{M}_{\odot}$. We additionally compare our weak lensing measurement to the virial mass derived using dynamical techniques, and find they are in agreement. This is the lowest redshift, largest angle weak lensing measurement of an individual cluster to date.

Subject headings: galaxies: clusters: individual(Coma) — gravitational lensing

1. Introduction

Measurements of the mass of the Coma cluster date back to Zwicky (1933) who first applied the virial theorem to Coma and showed that dark matter dominates the cluster on megaparsec scales. Since then a number of methods have been used to determine the mass of Coma under various assumptions. Kent & Gunn (1982) used the galaxy surface density profile to measure the mass under the assumption that the mass traces the galaxy distribution. The & White (1986) later used this dataset to measure the mass with a modified version of the virial theorem. Hughes (1989) used X-ray data under the assumption that the cluster is in hydrostatic equilibrium. More recently Geller et al. (1999) used the cluster infall region of Coma to extrapolate the mass out to $10h^{-1}$Mpc as well as to determine the virial mass.

[1]Center for Particle Astrophysics, Fermi National Accelerator Laboratory, Batavia, IL 60510

[2]Physics Department, Brown University, Box 1843, Providence, RI 02912

[3]Kavli Institute for Cosmological Physics and Department of Astronomy & Astrophysics, University of Chicago, Chicago, IL 60637

Weak lensing has become a powerful tool with which to measure the mass of galaxy clusters (Tyson et al. 1990). Here the shape distortion of background galaxies due to a foreground cluster is used to determine the mass of the cluster independent of dynamical assumptions. The shear induced on the background galaxies can be used to probe the mass of the foreground cluster out to large radii. The majority of galaxy clusters studied with weak lensing lie at redshift $z \geq 0.2$ (Dahle 2007). However lower redshift clusters have been probed using this method, for instance Joffre et al. (2000) studied Abell 3667 at $z = 0.055$. At very low redshifts weak lensing measurements of clusters become difficult since this requires imaging of a large area surrounding the cluster.

The possibility of a weak lensing study of the Coma Cluster ($z = 0.0236$) with the SDSS was first suggested by Gould & Villumsen (1994) and Stebbins et al. (1996). They pointed out that since Coma is at such a low redshift the weak lensing signal would be measurable in the SDSS since virtually all background galaxies would be at a much higher redshift than Coma. This is in spite of the shallow imaging in the SDSS which yields a typical background galaxy surface density of ~ 1 galaxy arcmin^{-2} (Sheldon et al. 2004). Complete imaging of the entire region surrounding the Coma Cluster was recently completed in the SDSS Data Release Five (Adelman-McCarthy et al. 2007).

Here we present a weak lensing measurement of the virial mass of the Coma Cluster in the SDSS. Our paper is organized as follows: in §2 we discuss our weak lensing analysis, in §3 our determination of the mass of Coma is discussed, and in §4 we compare our weak lensing mass estimate to previous measurements of the virial mass of Coma.

Since Coma is at such a low redshift our results do not change significantly for different density parameters. However for completeness we have assumed a standard cosmology with $\Omega_m = 0.3$ and $\Omega_\Lambda = 0.7$.

2. Weak Lensing Analysis

2.1. Data

Data used in our study are obtained from the Sloan Digital Sky Survey (SDSS) (York et al. 2000) a large imaging and spectroscopic survey of an 8000 square degree region in the Northern Galactic Cap centered on $\alpha = 12^{\rm h}22^{\rm m}$, $\delta = 32°13'$ (J2000). The SDSS uses a dedicated 2.5m telescope at Apache Point Observatory which images the sky in the *ugriz* bands (Fukugita et al. 1996) in a drift scan mode (Stoughton et al. 2002). The astrometric calibration of the SDSS is described in Pier et al. (2003) and the photometric calibration is described in Tucker et al. (2006) and Hogg et al. (2001). For our analysis we use the SDSS

Data Release Five (Adelman-McCarthy et al. 2007) which contains complete imaging of the region surrounding Coma.

Object detection and shape measurement are performed using the PHOTO pipeline (Lupton et al. 2001). PHOTO measures a large number of parameters for each detected object in the SDSS (Stoughton et al. 2002), including adaptive moments (Bernstein & Jarvis 2002) which we use to measure galaxy shapes. In the SDSS adaptive moments are measured using an iterative algorithm which adapts a Gaussian weight function to the size and shape of each galaxy (Sheldon et al. 2004). PHOTO convolves each image with the local PSF before detecting objects in order to avoid the selection bias described in Bernstein & Jarvis (2002). Drift scanning in the SDSS creates a time dependent PSF which leads to a spatial variation in image quality. To model the PSF in the SDSS a Karhunen-Loeve (KL) decomposition is used, described in further detail in Lupton et al. (2001) and Sheldon et al. (2004). Camera shear due to drift scanning in the SDSS has been previously shown to be small (Hirata et al. 2004).

For our weak lensing analysis we use a $\sim$ 200 square degree region centered on the core of the Coma Cluster. The core of Coma contains two bright cluster galaxies (BCGs) : NGC 4874 & NGC 4889. We take as the center of Coma the galaxy NCG 4874 located at $\alpha = 13^{\rm h}02^{\rm m}00.2^{\rm s}$, $\delta = 27^{\circ}41^{'}26.6^{''}$ (J2000). This BCG is associated with the majority of the X-ray flux in the core (Vikhlinin et al. 2001) and the large number of galaxies surrounding this BCG in the optical imaging is indicative of this being the center of the cluster potential (see e.g., Hansen et al. 2005). We in fact find that the shear amplitude is maximized when we use this BCG as the cluster center.

2.2. Source Galaxies

To create our source galaxy catalog we use only objects which have been detected in all three *gri* filters. We eliminate objects which contain saturated pixels, were originally blended with another object, or triggered errors in the measurement of adaptive moments by rejecting objects with the respective PHOTO error flag set. For our study we use only objects which have been classified by PHOTO as galaxies (type = 3). We additionally use only shape measurements from the r band since this filter is the most sensitive and typically contains better seeing (Adelman-McCarthy et al. 2007). Galaxies are selected in the r band with extinction corrected model magnitudes (Stoughton et al. 2002) in the range $18 < r < 21$ (Figure 1). Model magnitudes are used here instead of Petrosian magnitudes since these provide a higher S/N (Mandelbaum et al. 2005). Galaxies with fainter magnitudes have been used in galaxy-galaxy weak lensing studies in the SDSS (Sheldon et al. 2004), but here

we restrict our sample to the magnitude range where errors in shape measurements are typically small (Hirata et al. 2004) and galaxy sizes are larger.

In our analysis we use photometric redshifts for our source galaxies. The SDSS photometric redshift pipeline of Csabai et al. (2003) is used since it completely covers the area of Coma in Data Release Five. Galaxies in our magnitude range are typically at much higher redshift than Coma, but we use photometric redshifts here to aid in the rejection of fainter cluster members. For our study we use only galaxies with photometric redshifts in the range $0.2 < z_{\rm phot} < 0.8$ and redshift errors $z_{\rm err} < 0.4$. Galaxies with lower photometric redshifts are not used as the fractional error in redshift rapidly increases and most of the shear signal comes from galaxies at high redshifts compared to Coma.

To correct for the PSF anisotropy and dilution we use the linear PSF correction scheme of Hirata & Seljak (2003). This algorithm uses the measured galaxy ellipticity and reconstructed PSF at the position of the object to correct the ellipticity components of each galaxy. We use galaxies with corrected ellipticities $e_{\rm corr} < 1.4$ in our analysis, which is typical for weak lensing studies in the SDSS (Hirata et al. 2004). We additionally make a cut on the resolution parameter (R), defined as

$$R = 1 - \frac{M_{\rm rrcc}^{\rm PSF}}{M_{\rm rrcc}} \tag{1}$$

(Bernstein & Jarvis 2002) where $M_{\rm rrcc}$ is the size of the galaxy and $M_{\rm rrcc}^{\rm PSF}$ is the size of the PSF at the position of the galaxy as calculated by PHOTO. For our analysis we use only galaxies with $R > 0.33$, which is equivalent to only using objects 1.5 times larger than the PSF. We additionally rotate the PSF corrected ellipticity components of each galaxy from image coordinates to the equatorial coordinate system.

Within the annulus described in §2.3, the total number of galaxies in our source galaxy catalog after applying these cuts is $\sim 270,000$.

2.3. Shear Measurement

The shear due to Coma is measured by projecting the PSF corrected ellipticity components of each source galaxy to the tangential frame and binning the galaxies into radial annuli between $0.05{\rm h}^{-1}$Mpc and $10.5{\rm h}^{-1}$Mpc. The edge of the inner annulus is chosen to be larger than the Einstein radius of Coma ($\sim 30''$) to ensure we are outside of the strong lensing regime, and also to avoid contamination from the BCGs. Since our radial annuli extend out to $\sim 10{\rm h}^{-1}$Mpc ($\simeq 8^\circ$), we modify the usual flat sky shear matrix into a curved

sky shear matrix, following Castro et al. (2005). The tangential shear is measured using

$$\gamma_t = \frac{1}{2\mathcal{R}} \frac{\sum e_t}{N} \tag{2}$$

where γ_t is the tangential shear, e_t is the tangential ellipticity, N is the total number of objects in each radial bin, and $\mathcal{R}$ is the shear responsivity described in Bernstein & Jarvis (2002). We chose not to use any ellipticity error weighting here since our galaxies are selected in a magnitude range where source galaxy ellipticity error is typically small in the SDSS (Hirata et al. 2004). We additionally also chose not to weight each source galaxy by the critical surface mass density because all of our source galaxies are at a much higher redshift than Coma and therefore the weights are very nearly equal. In the case of no weights, the shear responsivity is $\mathcal{R} = 1 - \sigma_{\rm SN}^2$, where $\sigma_{\rm SN}$ is the shape noise (the width of the intrinsic ellipticity distribution per ellipticity component) (Wittman 2002). Here we use a shape noise of $\sigma_{\rm SN} = 0.37$ which was used previously in Hirata et al. (2004) for the same source galaxy magnitude range.

The resulting shear profile for Coma is shown in Figure 2. We expect to detect the shear out to $\sim 5{\rm h}^{-1}$Mpc, and the shear (solid squares) is clearly detected in these inner bins. Also shown in Figure 2 is a null test (open triangles) where each source galaxy is rotated by 45°. The shear signal should dissappear after this rotation if the signal is due to lensing. Errors shown for both quantities in Figure 2 are 1σ error bars, where σ is the standard deviation of the mean in each radial bin.

To statistically test the significance of our measured shear signal we test whether it is consistent with the null shear model ($\gamma_t = 0$). We find that our measured shear gives a $\chi^2 = 23.33$ for 6 degrees of freedom for the null model. The probability of obtaining a reduced $\tilde{\chi}^2$ greater than this value is $P(\tilde{\chi}^2 \geq \tilde{\chi}_o^2) = 0.07\%$, and therefore we can reject the null hypothesis. For comparison, fitting the shear from the 45° test to the null model gives a $\chi^2 = 5.65$ for 6 degrees of freedom, which is consistent with the null hypothesis.

2.4. Blank Fields Test

To test that our signal is not affected by any remaining systematic in the survey, we split up the SDSS North into separate, non-overlapping 'Coma sized' patches that contained no galaxies used in our Coma analysis and which contained no large sections of missing data. We were able to successfully extract 6 blank fields in DR5 each $\sim 20^\circ \times 20^\circ$ wide. From the center of each patch we probed radially outward to $\sim 10{\rm h}^{-1}$Mpc at the redshift of Coma. We applied the same cuts to the source galaxy catalog in each of the blank fields that were used in our Coma analysis in §2.2. The resulting inverse variance weighted average signal over all

fields is shown in Figure 3, where we have used the same binning as in our Coma analysis. The tangential shear signal is shown with solid squares and the 45° component is shown with open triangles. The tangential shear component is consistent with the null model giving a $\chi^2 = 1.84$ for 6 degrees of freedom. The 45° component gives a $\chi^2 = 12.58$ for 6 degrees of freedom which has a probability $P(\tilde{\chi}^2 \geq \tilde{\chi}^2_o) = 5.0\%$. A model with a small positive shear is slightly favored for the 45° component, however the null model can only be excluded at the 5% level. The field to field scatter in the blank field shear measurements shows a typical standard deviation in a given radial bin of $\sigma_\gamma \sim 0.0015$ or a standard deviation of the mean of ~ 0.0006, similar in magnitude to the statistical errors that are plotted in Figure 3. In principle the scatter over the blank fields can provide information on the error due to large scale structure (Hoekstra 2001; also §4.4 below), but our determination of the scatter is limited by the finite number of blanks fields.

3. Mass Model

3.1. Tangential Shear

The tangential shear due to a foreground cluster lens is given by

$$\gamma_t = \frac{\bar{\Sigma}(\leq r) - \Sigma(r)}{\Sigma_{\rm crit}} \tag{3}$$

where $\bar{\Sigma}(\leq r)$ is the average projected surface mass density interior to r, and $\Sigma(r)$ is the projected surface mass density at r (Miralda-Escude 1991). The magnitude of the shear also depends on the critical surface mass density $\Sigma_{\rm crit}$ which is determined by

$$\Sigma_{\rm crit} = \frac{c^2}{4\pi G}\frac{D_s}{D_l D_{ls}}. \tag{4}$$

Here D_l and D_s are the angular diameter distances from the observer to the lens and source respectively, and D_{ls} is the angular diameter distance between the lens and source.

To compute the critical surface mass density we use for the lens the exact spectroscopic redshift of Coma $z = 0.0236$ (Geller et al. 1999). We assume here that the peculiar velocity for Coma is zero, which has been shown in several studies (Scodeggio et al. 1997; Giovanelli et al. 1997). Photometric redshifts are used to calculate the source angular diameter distances, and we obtain a critical surface mass density of $26299 M_\odot pc^{-2}$. For comparison this is nearly the value obtained if we assume all of our sources were at a fixed redshift of $z = 0.3$.

3.2. NFW Profile

Since the S/N of our data is low ($S/N \sim 5$) we chose to fit the measured shear profile of Coma to a model. We fit the shear to that expected from a Navarro, Frenk, & White (NFW) profile (Navarro et al. 1996). The NFW profile is a "universal profile" found in N-body simulations to fit mass density profiles ranging from galaxies to galaxy clusters. The density of an NFW profile is described by

$$\rho(r) = \frac{\delta_c \rho_c}{(r/r_s)(1 + r/r_s)^2} \tag{5}$$

where δ_c is the halo overdensity, r_s is the scale radius, and $\rho_c = 3H^2(z)/8\pi G$ is the critical density at the redshift of the cluster. The halo overdensity is given by

$$\delta_c = \frac{200}{3} \frac{c^3}{\ln(1+c) - c/(1+c)} \tag{6}$$

where c is the halo concentration. The NFW model is therefore determined by only two parameters c and r_s which are highly correlated. The NFW model can be used to determine the virial radius $r_{200} = cr_s$ defined as the radius in which the interior mass density falls to $200\rho_c$. The corresponding virial mass M_{200} is given by

$$M_{200} = \frac{800\pi}{3} \rho_c r_{200}^3. \tag{7}$$

The expected shear due to an NFW profile has been worked out in detail by Wright & Brainerd (2000) and we use their result in our analysis. Because the NFW profile is highly non-linear, we use the Levenberg-Marquardt fitting procedure in Press et al. (1995) to determine the virial radius and the halo concentration. We find that the values which minimize χ^2 are given by

$$r_{200} = 1.99^{+0.21}_{-0.22} \mathrm{h}^{-1}\mathrm{Mpc} \tag{8}$$

and

$$c = 3.84^{+13.16}_{-1.84}. \tag{9}$$

The concentration parameter is not well constrained. This fit gives a $\chi^2 = 3.87$ for 4 degrees of freedom which has a $\mathrm{P}(\tilde{\chi}^2 \geq \tilde{\chi}_o) = 42.4\%$ probability of occuring. This corresponds to a virial mass of

$$M_{200} = 1.88^{+0.65}_{-0.56} \times 10^{15} \mathrm{M}_\odot. \tag{10}$$

Our values of r_{200} and M_{200} remain constant if the number of bins is slightly changed, and therefore our choice of binning does not bias this result. It has been shown previously that large scale structure affects the errors in the fit parameters of weak lensing measurements (Hoekstra 2003), however this is not considered in our fit errors. We discuss additional sources of systematic error not included in our fit in §4.4.

4. Discussion

We compare our weak lensing mass estimate with three other methods used to determine the virial mass of Coma: (1) The Virial Theorem (2) X-ray and (3) the Infall Region. Our value for M_{200} is consistently higher than the previous measurements, though never by more that 2σ. These comparisons are summarized in Table 1. We also discuss sources of additional error not included in our mass measurement, as well as the source of any potential bias.

4.1. Virial Theorem

The & White (1986) used a sample of galaxies in Coma along with the virial theorem to measure its mass. Their analysis also accounted for an additional portion of the system that may have been missing in their spectroscopic sample. Relaxing the assumption that light traces mass in the system, they found that the mass varied over a wide range. However, assuming that the mass traces the galaxy distribution they found a mass within $2.7\mathrm{h}^{-1}\mathrm{Mpc}$ of $0.95 \times 10^{15}\mathrm{h}^{-1}\mathrm{M}_{\odot}$ with a 15% error in mass. Our weak lensing measurement is consistent with this result to within $\sim 1.6\sigma$.

4.2. X-ray

Our weak lensing measurement is also consistent with the previous X-ray analysis of Hughes (1989). This study used the assumption of hydrostatic equilibrium but avoided certain assumptions about the state of the gas and also accounted for many systematic effects. The best fit model was one in which mass traces light, giving a virial mass of $(0.93 \pm 0.12) \times 10^{15}\mathrm{h}^{-1}\mathrm{M}_{\odot}$ within $2.5\mathrm{h}^{-1}\mathrm{Mpc}$ which is within $\sim 1.7\sigma$ of our result.

4.3. Infall Region

Using a redshift survey of $\sim$ 1000 galaxies Geller et al. (1999) used the infall region of Coma to determine its mass. In redshift space galaxies falling into the potential well of the cluster are used to determine the amplitude of the redshift caustics (the boundaries in line of sight velocity vs. projected radius) (Diaferio & Geller 1997). The amplitude of the caustics along with the assumptions of spherical symmetry and hierarchal clustering are directly related to the cluster gravitational potential. Using this technique they find an NFW model fits the mass well giving an estimate for $r_{200} = 1.5\mathrm{h}^{-1}\mathrm{Mpc}$ which yields an

$M_{200} = 0.8 \times 10^{15} M_{\odot}$. Error bars are not quoted for their virial radius or mass; however, our weak lensing virial mass is in agreement with their central result to within $\sim 2.0\sigma$

4.4. Additional Error and Bias

Weak lensing measurements of the mass of clusters, in particular low redshift clusters, suffer from two sources of additional error: (1) distant large scale structure and (2) correlated structure near the cluster (Hoekstra 2003). Weak lensing is sensitive to all structure along the sight and it has been shown that any background structure introduces additional error in the weak lensing mass estimate of clusters (Hoekstra 2001). Specifically for the case of the Coma Cluster, Hoekstra (2001) showed that the error due to large scale structure increases with imaging depth, thus limiting the total achievable S/N for Coma to ~ 7. In our study the imaging depth in SDSS is relatively shallow so the contribution of large scale structure to the total error budget is small. For future deep imaging surveys which will also cover the area of Coma such as PanSTARRS (Kaiser et al. 2002), the error due to large scale structure will be more significant.

The effect of correlated structure (such as filaments) near a foreground cluster has been previously studied using N-body simulations by Cen (1997) and Metzler et al. (1999). Here it was shown that filaments can increase the statistical error in weak lensing mass estimates as well as cause the measured M_{200} to be biased toward higher values. In principle Coma should be an interesting testing ground to study this effect since the neighboring structure is well understood. However in practice there is not a clear method to correct a weak lensing measured value of M_{200} for this effect, and therefore we leave a study of any potential bias in our measurement for a future paper.

5. Conclusion

We have measured the weak lensing shear due to the Coma Cluster, currently the lowest redshift ($z = 0.0236$) largest angle weak lensing measurement of an individual cluster to date. Our analysis is performed using the SDSS which is the only imaging survey that covers a large enough area to measure the shear due to Coma. We find the shear can be fit well to an NFW profile and have compared our weak lensing derived mass estimate to dynamical methods which have been used to probe the mass of Coma out to large radius. In particular we have compared our weak lensing mass to the mass derived using the virial theorem (The & White 1986), X-ray data (Hughes 1989), and the cluster infall region (Geller et al. 1999). We find

the virial mass of Coma from weak lensing is consistent with the mass derived using these other techniques, though the error from weak lensing is larger.

We thank the Fermilab Clusters Group for useful comments during the course of this work. Funding for the SDSS and SDSS-II has been provided by the Alfred P. Sloan Foundation, the Participating Institutions, the National Science Foundation, the U.S. Department of Energy, the National Aeronautics and Space Administration, the Japanese Monbukagakusho, the Max Planck Society, and the Higher Education Funding Council for England. The SDSS Web Site is http://www.sdss.org/.

The SDSS is managed by the Astrophysical Research Consortium for the Participating Institutions. The Participating Institutions are the American Museum of Natural History, Astrophysical Institute Potsdam, University of Basel, University of Cambridge, Case Western Reserve University, University of Chicago, Drexel University, Fermilab, the Institute for Advanced Study, the Japan Participation Group, Johns Hopkins University, the Joint Institute for Nuclear Astrophysics, the Kavli Institute for Particle Astrophysics and Cosmology, the Korean Scientist Group, the Chinese Academy of Sciences (LAMOST), Los Alamos National Laboratory, the Max-Planck-Institute for Astronomy (MPIA), the Max-Planck-Institute for Astrophysics (MPA), New Mexico State University, Ohio State University, University of Pittsburgh, University of Portsmouth, Princeton University, the United States Naval Observatory, and the University of Washington.

REFERENCES

Adelman-McCarthy, J., et al. 2007, arXiv:0707.3380

Bernstein, G.M. & Jarvis, M.J. 2002, AJ, 123, 583

Castro, P.G., Heavens, A.F., Kitching, T.D. 2005, Phys. Rev. D, 72, 023516

Cen, R. 1997, ApJ, 485, 39

Dahle, H. 2007, preprint (astro-ph/0701598)

Diaferio, A., & Geller, M.J. 1997, ApJ, 481, 633

Csabai, I., et al. 2003, AJ, 125, 580

Fukugita, M., Ichikawa, T., Gunn, J.E., Doi, M., Shimasaku, K., & Schneider, D.P. 1996, AJ, 111, 1748

Geller, M. J., Diaferio, A., Kurtz, M.J. 1999, ApJ, 517L, 23

Giovanelli, R., Haynes, M.P., Herter, T., da Costa, L.N., Wolfram, F., Salzer, J.J., Wegner, G., 1997, AJ, 113, 53

Gould, A. & Villumsen, J. 1994, ApJ, 428L, 45

Hansen, S.M., McKay, T.A., Wechsler, R.H., Annis, J., Sheldon, E.S., Kimball, A. 2005, ApJ, 633, 122

Hirata, C.M. 2004, MNRAS, 353, 529

Hirata, C.M. & Seljak, U. 2003, MNRAS, 343, 459

Hoekstra, H. 2001, A&A, 370, 743

Hoekstra, H. 2003, MNRAS, 339, 1155

Hogg, D.W., Finkbeiner, D.P., Schlegel, D.J., & Gunn, J.E. 2001, AJ, 122, 2129

Hughes, J.P, 1989, ApJ, 337, 21

Joffre, M. et al. 2000, ApJ, 534L, 131

Kaiser, N. et al. 2002, SPIE, 4836, 154

Kent, S.M. & Gunn, J.E. 1982, AJ, 87, 945

Lupton, R., Gunn, J., Ivezic, Z., Knapp, G.R. 2001, preprint (astro-ph/0101420)

Mandelbaum, R., et al. 2005, MNRAS, 361, 1287

Metzler, C.A., White, M., Norman, M., Loken, C. 1999, ApJ, 520L, 9

Miralda-Escude, J. 1991, ApJ, 370, 1

Navarro, J.F., Frenk, C.S., White, S.D. 1996, ApJ, 462, 563

Pier, J.R., et al. 2003, AJ, 125, 1559

Press, W.H., Flannery, B.P., Teukolsky, S.A., Vetterling, W.T. 1995, Numerical Recipes in C (2nd ed.; Cambridge:Cambridge Univ. Press)

Scodeggio, M., Giovanelli, R., & Haynes, M.P., 1997, AJ, 113, 101

Sheldon, E.S., 2004, AJ, 127, 2544

Stebbins, A., Mckay, T., Frieman, J.A., 1996, in IAU Symp. 173, Astrophysical Applications of Gravitational Lensing, ed.s C.S. Kochanek and J.N. Hewitt (Kluwer Academic, New York), 75

Stoughton, C., et al. 2002, AJ, 123, 485

The, L.S., & White, S.D. 1986, AJ, 92, 1248

Tucker, D.L., et al., 2006, AN, 327, 821

Tyson, J.A., Wenk, R.A., & Valdes, F. 1990, ApJ, 349L, 1

Vikhlinin, A., Markevitch, M., Forman, W., Jones, C. 2001, ApJ, 555L, 87

Wittman,D. 2002, LNP, 608, 55

Wright, C.O. & Brainerd, T.G. 2000, ApJ, 534, 34

York, D.G., et al. 2000, AJ, 120, 1579

Zwicky, F. 1933, Helvetica Phys. Acta, 6, 110

Table 1. Virial Mass Estimates of Coma

Virial Radius (h^{-1}Mpc)	Mass ($10^{15}h^{-1}M_{\odot}$)	Reference
$1.99^{+0.21}_{-0.22}$	$1.88^{+0.65}_{-0.56}$	this work[a]
1.5	0.8	1[a]
2.5	0.93 ± 0.12	2
2.7	0.95 ± 0.15	3

[a]Determined from the NFW r_{200} virial radius.

References. — (1) Geller et al. 1999; (2) Hughes 1989; (3) The & White 1986.

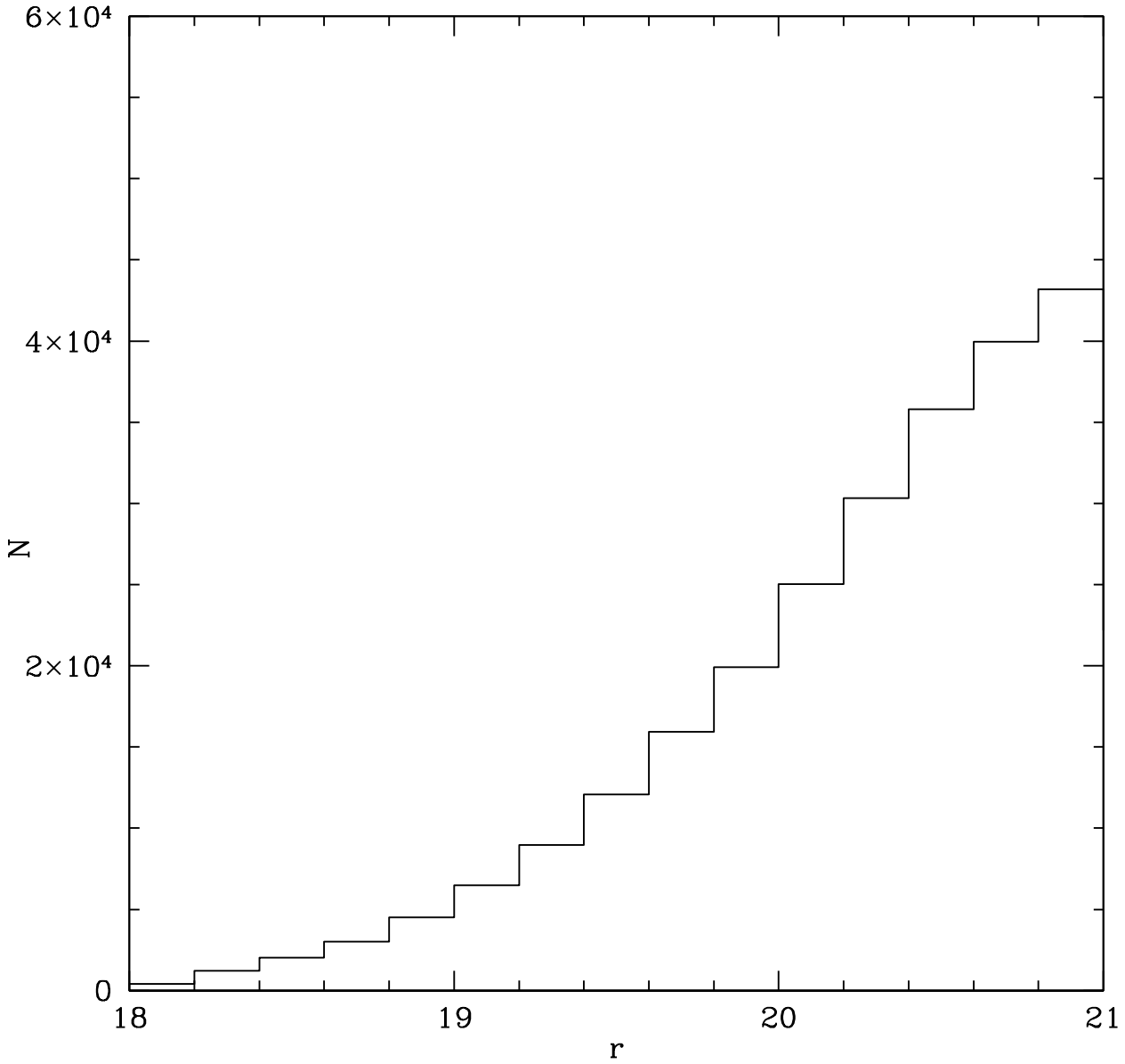

Fig. 1.— r band magnitude distribution of source galaxies used in our analysis. Objects with extinction corrected model magnitudes between $18 < r < 21$ are used. The total number of source galaxies used to measure the shear due to Coma is $\sim 270,000$.

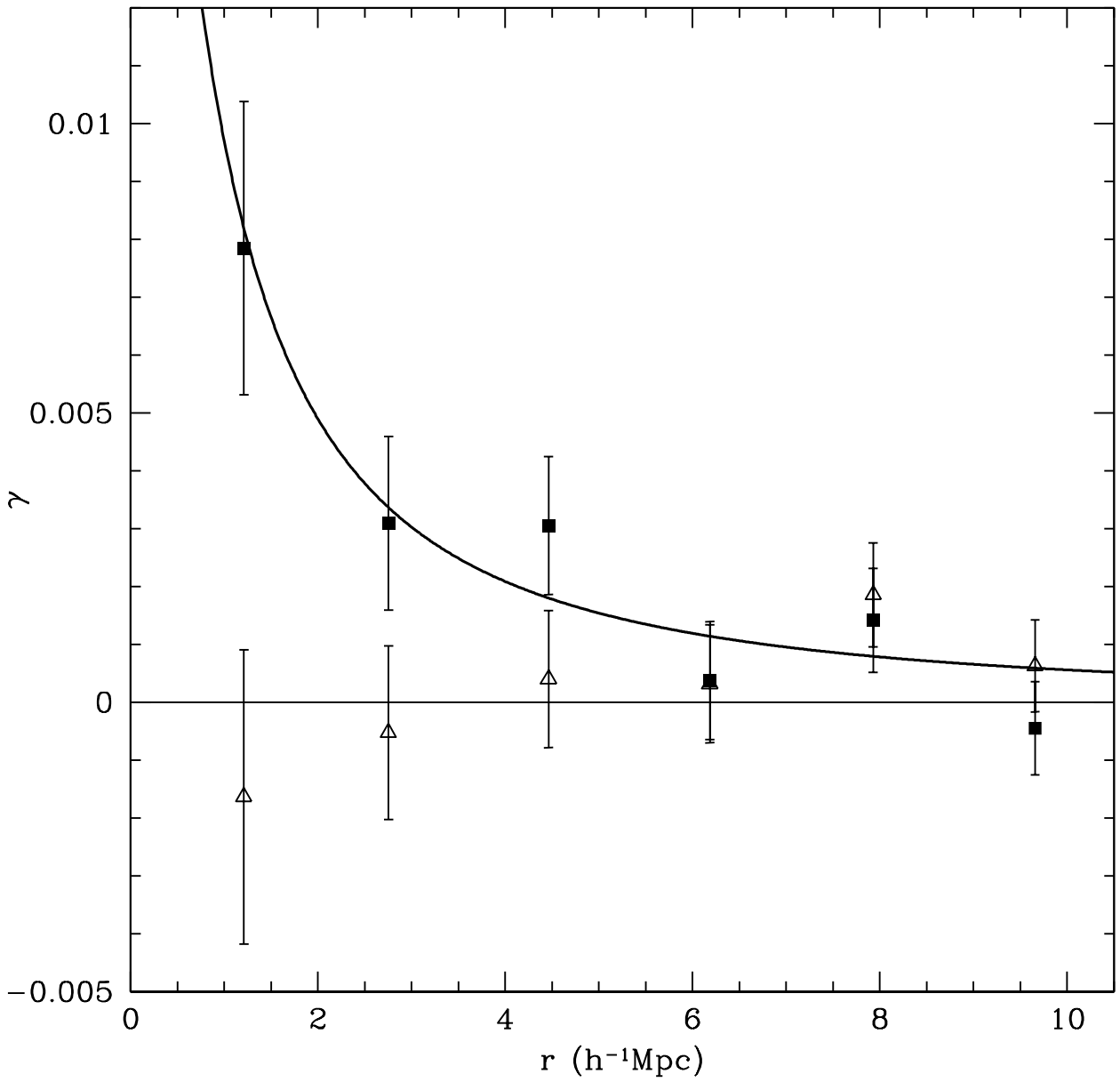

Fig. 2.— Tangential shear centered on the Coma Cluster in the SDSS. The measured shear is shown as *solid squares* along with 1σ error bars. The 45° component is shown as *open triangles* and is consistent with zero. The *solid line* represents our best fit NFW model.

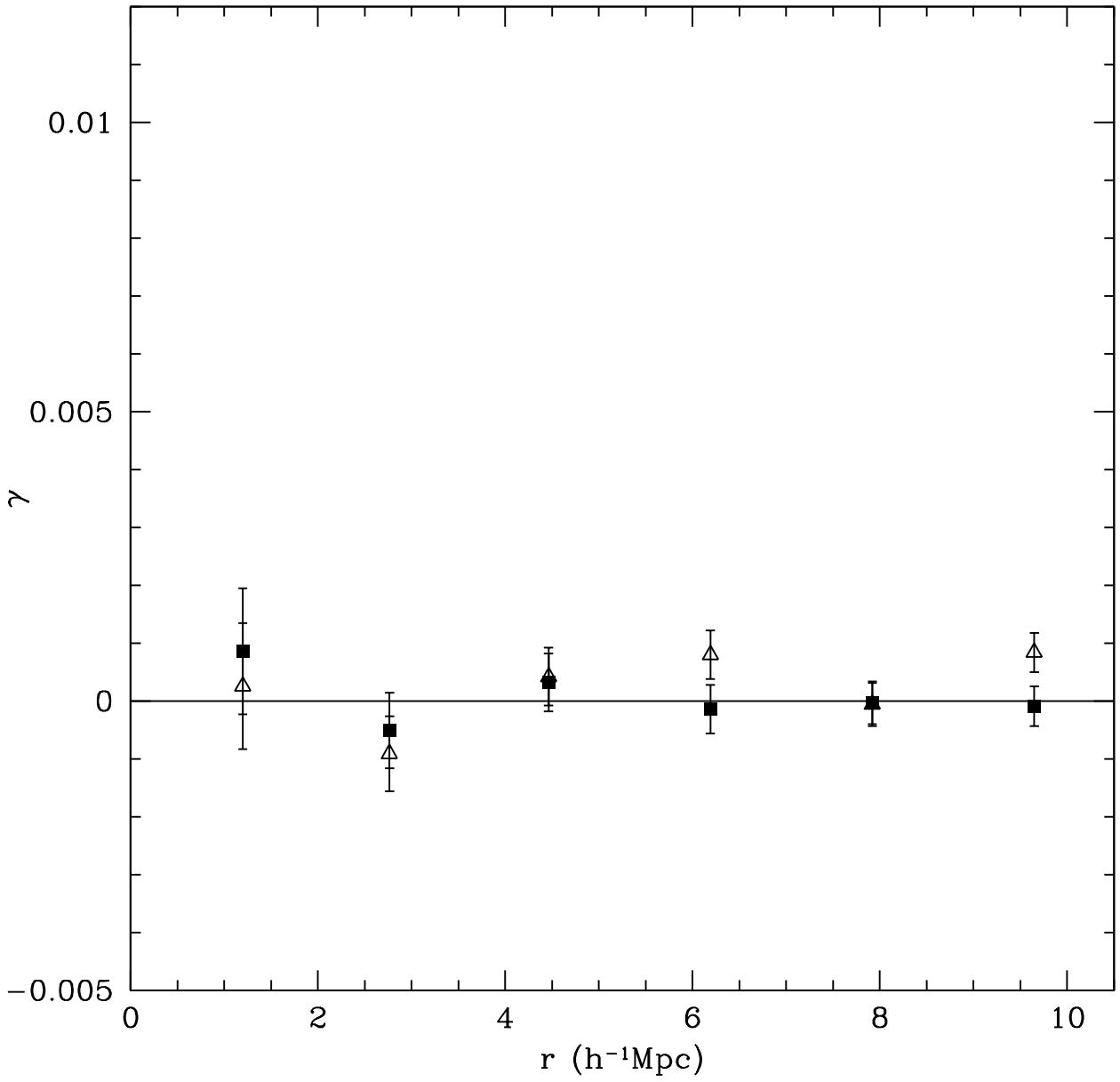

Fig. 3.— Average tangential shear measured from "blank" regions of the SDSS North not associated with Coma. The shear signal (*solid squares*) and 45° component (*open triangles*) should be zero in these regions. Results are the inverse variance weighted average of 6 independent $\sim 20^\circ \times 20^\circ$ patches. The size of the annuli here match those used to evaluate the shear due to Coma.